Renewable and Sustainable Energy Reviews 34 (2014) 525–535

Contents lists available at ScienceDirect

Renewable and Sustainable Energy Reviews

journal homepage: www.elsevier.com/locate/rser

Study on modelling microalgae growth in nitrogen-limited culture system for estimating biomass productivity

Shuo Yuan [a], Xinping Zhou [a,*], Ranchi Chen [b], Bao Song [c]

[a] Department of Mechanics, Huazhong University of Science and Technology (HUST), Wuhan 430074, China
[b] School of Mechanical Engineering, Purdue University, West Lafayette, IN 47906, USA
[c] School of Mechanical Science and Engineering, HUST, Wuhan 430074, China

ARTICLE INFO

Article history:
Received 19 July 2013
Received in revised form
13 February 2014
Accepted 12 March 2014
Available online 3 April 2014

Keywords:
Microalgae growth
Modelling
Biomass productivity
Nitrogen-limited

ABSTRACT

Microalgae are considered as a promising biofuel resource to fix carbon dioxide (CO_2) in the future. Modelling microalgae growth is an effective method of studying the performance of microalgae growth manifested by the parameters including light distribution, pigment dynamics, nitrogen uptake, growth rate, respiration rate, temperature dependence, and depth dependence, and helping to control the culture of microalgae in artificial bioreactors. In this paper, the models of microalgae growth in nitrogen-limited and light-limited culture system for estimating biomass productivity are investigated by comparing different expressions and coefficients used in several main models. The results show that there are some differences among the results of numerical modelling due to different expressions and coefficients. This paper will lay a foundation for the selective use of microalgae growth models for researchers.

Contents

1. Introduction . . . 526
 1.1. Characteristics of microalgae . . . 526
 1.2. Microalgae models . . . 526
2. Model description . . . 526
 2.1. Bernard's model . . . 526
 2.2. Light distribution modelling . . . 527
 2.3. Pigment dynamics modelling . . . 527
 2.4. Nitrogen uptake modelling . . . 527
 2.5. Growth rate modelling . . . 528
 2.6. Respiration rate and degradation rate modelling . . . 528
 2.7. Depth dependence modelling . . . 528
 2.8. Temperature dependence modelling . . . 528
3. Results and discussion . . . 529
 3.1. Light distribution modelling . . . 529
 3.2. Pigment dynamics modelling . . . 530
 3.3. Nitrogen uptake modelling . . . 530
 3.4. Growth rate modelling . . . 530
 3.5. Respiration rate modelling . . . 531
 3.6. Depth dependence modelling . . . 532
 3.7. Temperature dependence modelling . . . 533
4. Conclusions . . . 534
Nomenclature . . . 534

* Corresponding author. Tel.: +86 27 8754 3838.
E-mail address: xpzhou08@hust.edu.cn (X. Zhou).

http://dx.doi.org/10.1016/j.rser.2014.03.032
1364-0321/

Acknowledgement . . . 535
References . . . 535

1. Introduction

1.1. Characteristics of microalgae

With the continuous reduction of the fossil fuels, and the acceleration of global greenhouse effect mainly due to carbon dioxide (CO_2) emissions, energy supply may be in trouble in the near future. It is urgent and significant to find reliable clean energy resources alternative to fossil fuels [1]. Microalgae may become one of the most promising new resources to supply energy and mitigate CO_2 in the future [2,3]. Technologies for producing microalgae and using microalgae for biodiesel have been known for more than 50 years. Up to now, many researchers have done plenty of work on planktons [4–7]. Compared to the first generation biofuels, microalgae have several advantages in sustainability, economics and environment. Microalgae not only have higher productivity, but also can be fed in saline/brackish water/coastal seawater on non-arable and deserted land. However, there are some shortcomings of microalgae for use as biofuels. For example, the dry solids content of the microalgae and water mixture can be as low as 0.05% dry solids content. The energy balance associated with segregating the water from the microalgae dry solids to allow a bio-esterification process to be undertaken is very high [8]. Literature [9] also indicated that some unstable biodiesel with many polyunsaturates will be derived in the process of producing biodiesels from algae oil.

1.2. Microalgae models

Some models have been established by various researchers to predict different aspects of microalgae growth process, such as mass growth, light distribution, pigment dynamics, nitrogen uptake, depth dependence, temperature dependence and respiration rate, etc. [10–13]. The biological model of microalgae comes from the population model proposed by Malthus [14]. The concept of the population model such as growth rate is used in later microalgae growth models. Droop [15,16] proposed a dynamic model which takes the dilution rate and influent inorganic nitrogen concentration into account to describe the growth of microalgae. The model is classical, but practical, which describes the kinetic model of the algae growth and the nitrogen uptake. Recently, several new models were proposed based on Droop's model. Geider et al. [17] proposed a new model which included growth process, nitrogen uptake, chlorophyll synthesis, temperature and respiration aspects, but depth dependence was ignored. Quinn et al. [18] proposed a model for industrial scale systems based on Geider et al.'s model [17]. A dynamic model was proposed by Packer et al. [19] to predict the growth and neutral lipid synthesis of green algae by using a new method. This method considered the influences of two factors (i.e., the photosynthesis, and the nitrogen uptake) on the growth rate, which was defined as a piecewise function of the two factors. Bernard [20] proposed a different kinetic model which was verified by experimental data [21]. Different from Packer et al.'s model [19], the light-limited and nitrogen-limited factors will simultaneously have effects on the growth rate in the model. Mairet et al. [22] further developed the previous models by dividing the biomass into three compartments including the function part, carbohydrates, and neutral lipids. The transformations and balances between the three parts were discussed in their model.

In the above models, various expressions and coefficients have been used. Investigation on the differences between them is needed so that it is easier for later researchers to select more proper expressions and coefficients to model, predict and control the microalgae growth. By now, little work on the comparison of different microalgae sub-models (that is, the expressions or coefficients, for example, the sub-model of nitrogen uptake) has been reported. In this paper, based on the valid Bernard's dynamic model [20] acting as the basic model (not the standard model) made up of several sub-models, various expressions and coefficients in several main models [17–19] will be compared by comparing the basic model and a new model. The new model is produced when one sub-model of the basic model is replaced by the corresponding sub-model used in another model. In the second and the third parts, the influence of other aspects such as the depth of culture and the ambient temperature is also discussed.

2. Model description

Many models have been proposed up to now, which used various expressions to calculate the parameters e.g. light distribution, pigment dynamics, nitrogen uptake, growth rate, respiration rate, and temperature dependence. In this part, we will describe Bernard's model, and the various expressions of parameters for various models [17–20] are also discussed.

2.1. Bernard's model

The model [20] describes four variables in the ordinary differential equations: $s(t)$, which denotes the concentration of dissolved inorganic nitrogen, the nitrate or ammonium ($\mathrm{g\,N\,m^{-3}}$), $q(t)$, which is internal nitrogen cell quota ($\mathrm{g\,N\,(g\,C)^{-1}}$), $x(t)$ which is algae biomass concentration ($\mathrm{g\,C\,m^{-3}}$), and $I^*(t)$ which is not the real radiation but a conceptual variable denoted radiation. The unit of $I^*(t)$ is $\mathrm{mol\,m^{-2}\,s^{-1}}$, which means the number of photons absorbed per unit area per unit time. The expression of calculating variable I^* will be discussed later. The four ordinary differential equations were expressed as:

$$\dot{s} = Ds_{in} - \overline{\rho}\frac{s}{s+K_s}\left(1-\frac{q}{Q_1}\right)x - Ds \tag{1}$$

$$\dot{q} = \overline{\rho}\frac{s}{s+K_s}\left(1-\frac{q}{Q_1}\right) - \overline{\overline{\mu}}(I_0, I^*, x, q)(q-Q_0) \tag{2}$$

$$\dot{x} = \overline{\overline{\mu}}(I_0, I^*, x, q)\left(1-\frac{Q_0}{q}\right)x - Dx - Rx \tag{3}$$

$$\dot{I}^* = \overline{\overline{\mu}}(I_0, I^*, x, q)\left(1-\frac{Q_0}{q}\right)(\overline{I}-I^*) \tag{4}$$

where D denotes the dilution rate, $\overline{\rho}$ is the maximum nitrogen uptake rate, S_{in} is influent inorganic nitrogen concentration, R is the inspiration rate, $\overline{I}$ is the average radiation along culture volume, Q_0 is the minimum nitrogen quota, Q_1 is the maximum nitrogen quota, and $\overline{\overline{\mu}}$ denotes the average growth rate, which is calculated by

$$\overline{\overline{\mu}}(I_0, \xi) = \tilde{\mu}\frac{2K_{il}}{\lambda\sqrt{\Delta}}\arctan\left(\frac{I_0(1-e^{-\lambda})\sqrt{\Delta}}{2I_0^2e^{-\lambda}+I_0(1+e^{-\lambda})K_{il}+2I_{opt}^2(\theta_0^C)}\right) \tag{5}$$

where I_0 represents the light intensity on the bioreactor surface, and $\tilde{\mu}$ is the maximum growth rate. The average radiation along culture volume $\bar{I}$ is given by

$$\bar{I} = \frac{I_0}{\lambda}(1 - e^{-\lambda}) \tag{6}$$

where the optical depth, λ, is the product of the depth of the culture L multiplied by light attenuation rate ξ

$$\lambda = \xi L \tag{7}$$

The light attenuation rate ξ can be calculated by

$$\xi = aChl + bx + c \tag{8}$$

where, a, b, and c are the constants, and the chlorophyll concentration Chl can be calculated by

$$Chl = \gamma(I^*)xq \tag{9}$$

The proportion of chlorophyll concentration to nitrogen concentration $\gamma(I^*)$ can be given by

$$\gamma(I^*) = \gamma_{\max}\frac{k_{I^*}}{I^* + k_{I^*}} \tag{10}$$

where $\gamma_{\max}$ is the maximum value of $\gamma(I^*)$.

The parameters Δ and I_{opt} which denote the radiation providing maximum rate of photosynthesis in Eq. (5) are calculated by

$$\Delta = 4I_{opt}^2(\theta_0^C) - K_{il}^2 \tag{11}$$

$$I_{opt} = \sqrt{K_{sI}K_{il}} \tag{12}$$

where K_{sI} is

$$K_{sI} = \frac{K_{sI}^*}{\theta_0^C} \tag{13}$$

The initial value of Chl/x is denoted by a parameter θ_0^C

$$\theta_0^C = \frac{Chl_0}{x_0} \tag{14}$$

where Chl_0 is the initial value of Chl, and x_0 is the initial value of x.

2.2. Light distribution modelling

Light intensity is an important factor of the algae growth model [23]. In nearly all the models, the Lambert–Beer Law was used to describe the light distribution in the reactor. The law assumes that the light below the culture surface is attenuated at an exponentially decaying rate because the biomass and/or the chlorophyll absorb a part of the radiation from the culture surface

$$I(L) = I_0 e^{-\xi L} \tag{15}$$

Eq. (6) can be obtained from Eq. (15). The exponential factor of light attenuation in the culture, ξ, may be related to the biomass content and/or the chlorophyll content. There are four different expressions of calculating ξ: (1) $a \neq 0, b \neq 0, c = 0$, that is, the factor ξ depends on both the biomass concentration and the chlorophyll concentration, as reported by [20]; (2) $a = b = 0$, $c \neq 0$, that is, parameter $\xi \equiv c$ when the reactor depth L is not too deep, as reported by [17]; (3) $b \neq 0$, $a = c = 0$, that is, the light attenuation rate linearly correlated to biomass concentration, as reported by [18,24]; and (4) $a \neq 0$, $b = c = 0$, that is, light attenuation coefficient ξ is linearly related to chlorophyll content, as reported by [11,19].

2.3. Pigment dynamics modelling

Besides the known a, b, and c constants, the chlorophyll concentration in the reactor must be known for calculating the light attenuation coefficient. Bernard [20] assumed that the chlorophyll concentration is proportional to the nitrogen concentration, $x \times q$, as demonstrated by Eq. (9). The proportional coefficient is calculated with Eq. (10). Quinn et al. [18] considered $a = 0$ in Eq. (8). It is not necessary to calculate the chlorophyll content for calculating the light attenuation coefficient. Several other methods were also used to calculate the chlorophyll content.

(1) From Geider et al.'s model

In this model [17], the chlorophyll content is calculated with the following differential equation

$$\frac{1}{Chl}\frac{dChl}{dt} = \frac{h_{Chl}\rho}{\theta^C} - r_{Chl} \tag{16}$$

where ρ is the uptake rate of nitrogen, θ^C is the ratio of chlorophyll a to phytoplankton carbon, r_{Chl} is the chlorophyll a degradation rate constant, and h_{Chl} is the chlorophyll a synthesis regulation term, which is calculated by

$$h_{Chl} = \theta_{\max}^N \frac{x}{\alpha^{Chl}\theta^C I_0} \tag{17}$$

where θ^N is the ratio of chlorophyll a to N, $\theta_{\max}^N$ is the maximum value of θ^N, and α^{Chl} is the chlorophyll a—specific initial slope of the photosynthesis-light curve.

(2) From Packer et al.'s model

The model [19] used the chlorophyll quota θ^C to calculate the chlorophyll content

$$\theta^C = C_0\frac{\mu}{p}\theta^N\rho - \theta^C\mu \tag{18}$$

where C_0 is the carbon subsistence quota, and p is the photosynthesis rate. Eq. (18) didn't take the respiration into account.

2.4. Nitrogen uptake modelling

Nitrogen is an important material in microalgae culture. The nitrogen source in bioreactors can be inorganic source such as ammonium or nitrate and organic source. Microalgae can synthesize proteins and neutral lipids by absorbed nitrogen. It is necessary to model the nitrogen uptake. In Bernard's model [20] and Packer et al.'s model [19], the nitrogen uptake behavior was described with Eq. (2). Then a brief introduction to the origin of Eq. (2) will be given.

The nitrogen cell quota of the culture, q, is equal to the ratio of the nitrogen concentration to the carbon concentration. This is analogous to the C:N ratio which is of crucial importance to the digestibility of substrates. q can be expressed as:

$$q = \frac{s}{x} \Rightarrow \dot{q} = \frac{\dot{s}x - \dot{x}s}{x^2} = \frac{\dot{s}}{x} - \frac{\dot{x}}{x}s = \rho(s,q) - \mu(I_0, q, \xi)q \tag{19}$$

where $s = x \times q$, and μ is the growth rate. q changes due to the nitrogen uptake and the microalgae growth. The right side of Eq. (19) can be divided into two parts: the nitrogen uptake part $\rho(s,q)$ and the growth dilution part $\mu(I_0, q, \xi)q$

$$\rho(s,q) = \bar{\rho}\frac{s}{s + K_s}\left(1 - \frac{q}{Q_1}\right) \tag{20}$$

$$\mu(I_0, q, \xi) = \bar{\bar{\mu}}(I_0, \xi)\left(1 - \frac{Q_0}{q}\right) \tag{21}$$

where $\bar{\rho}$ is the maximum nitrogen absorption rate. Substituting Eqs. (20) and (21) into Eq. (19), Eq. (2) is derived. Then several methods to model the nitrogen uptake are shown:

(1) From Geider et al.'s model
In this model [17], Nitrogen uptake is described with a differential equation.

$$\dot{q}=\frac{\rho}{q}-r_N \tag{22}$$

$$\rho=\bar{\rho}\frac{s}{s+K_s}\left(\frac{Q_1-q}{Q_1-Q_0}\right)f(T) \tag{23}$$

where r_N is the remineralization rate constant, and $f(T)$ denotes the temperature function.

(2) From Quinn et al.'s model
In this model [18], the temperature function $f(T)$ has been considered. The equation of nitrogen uptake in Quinn et al.'s model is

$$\dot{q}=\bar{\rho}\frac{s}{s+K_s}\left(1-\frac{Q_0}{q}\right)f(T)-R_N \tag{24}$$

where R_N is the respiration constant for nitrogen.

2.5. Growth rate modelling

It is universally acknowledged that the growth rate is correlating to the radiation intensity. In Bernard's model, the nitrogen-limited and the light-limited are two multiplication factors, as shown by Eqs. (5) and (21). Eqs. (5) and (11)–(14) are used to calculate the growth rate of microalgae. There were some methods to calculate the microalgae growth rate in various models. Some models considered the light radiation effects on photosynthesis rate, others (e.g. Packer et al.'s model [19] and Bernard's model [20]) related the growth rate to the radiation intensity directly. In Packer et al.'s model [19], the growth rate was determined by both photosynthesis rate and the nitrogen uptake rate.

(1) From Geider et al.'s model
Geider et al. [17] assumed that the growth rate is the result of subtracting the energy consumption from the photosynthesis

$$\mu=\frac{1}{x}\frac{dx}{dt}=p-R_C-\zeta\rho \tag{25}$$

$$p=p_m\left[1-\exp\left(\frac{-\alpha^{Chl}\theta^C I_0}{P_m}\right)\right] \tag{26}$$

$$p_m=p^C_{ref}\left(\frac{q-Q_0}{Q_1-Q_0}\right) \tag{27}$$

where R_C is the maintenance respiration rate, ζ is the cost of biosynthesis, p_m is maximum value of p at temperature T, and p^C_{ref} is maximum photosynthesis rate. This model assumed that 50% of the biomass is carbon.

(2) From Quinn et al.'s model
Quinn et al.'s model [18] is the same as the Geider et al.'s one [17] except the use of different method to calculate p_m

$$p_m=p^C_{ref}\left(1-\frac{Q_0}{q}\right) \tag{28}$$

The nitrogen uptake factors expressions in Eqs. (27) and (28) are different. After comparing the variations of the values of $(q-Q_0)/(Q_1-Q_0)$ term in Eq. (27) and the values of $(1-Q_0/q)$ term in Eq. (28) with nitrogen quota q varying from 0.05 g N $(\text{g C})^{-1}$ to 0.25 g N $(\text{g C})^{-1}$, it is found out that the nitrogen uptake factor in Eq. (27) linearly increases from 0 to 1, and that in Eq. (28) logarithmically increases from 0 to 0.8.

(3) From Packer et al.'s model
The growth rate is interestingly shown as a piecewise function of time. The microalgae growth rate is determined by both nitrogen and light factors. The growth rate is therefore considered to be the minimum of the growth rates calculated by using the nitrogen-limited and light-limited relationships [19].

$$\dot{x}=\mu x-Dx \tag{29}$$

$$\mu=\min\left\{\tilde{\mu}\left(1-\frac{Q_0}{q}\right),\frac{p}{C_0}\right\} \tag{30}$$

$$p=\theta^C p_m\left[1-\exp\left(\frac{-A\Phi\bar{I}}{p_m}\right)\right] \tag{31}$$

$$p_m=\frac{(qx)^2 p^C_{ref}}{(qx)^2+(Q_0x)^2} \tag{32}$$

where the value of p^C_{ref} is selected to be 7 day^{-1} in Eq. (32), A is the optical cross section of chlorophyll a, C_0 is the carbon subsistence quota, $\tilde{\mu}$ is 3.26 day^{-1} in Eq. (30), and Φ is the Quantum efficiency.

2.6. Respiration rate and degradation rate modelling

There are five sub-models to model the respiration or the degradation of microalgae. In Bernard's model [20], respiration is taken into account only in the growth modelling. Quinn et al. [18] proposed a complex method to distinguishing two forms of respiration: respiration of growth, R_C, and the reapiration of nitrogen uptake, R_N. The two parameters R_N and R_C are used in Eqs. (24) and (25) to represent the two forms of respiration.

In Geider et al.'s model [17], three respiration or degradation rates, chlorophyll a degradation rate constant, r_{Chl}, nitrogen remineralization rate constant, r_N, and R_C were used. The three rates are equivalent, $R_C=r_N=r_{Chl}=0.025$ day^{-1}, which are used in Eqs. (16), (22) and (25), respectively.

The respiration or degradation rate is considered as a constant in all the above sub-models. Mairet et al. [22] didn't regard it as a constant respiration rate, but defined the respiration rate proportion by using a linear relationship to the nitrogen uptake rate ρ

$$R=r_0+r_1\rho(s,q) \tag{33}$$

where r_0 and r_1 are the coefficients.

2.7. Depth dependence modelling

In massive production, depth is a vital parameter in bioreactors such as in raceway or pond. If the bioreactors are deeper, more light radiation can be available for use, but more materials will be wasted. The influence of the variable depth will be discussed in next part.

2.8. Temperature dependence modelling

The function related to temperature T consists of two equations which were proposed by Quinn et al. [25].

$$f(T)=\frac{2\Phi_T}{(1+\Phi_T^2)} \tag{34}$$

$$\Phi_T=e^{\frac{E_a}{R_0T_{opt}}-\frac{E_a}{R_0T}} \tag{35}$$

where, R_0 is the universal gas constant, T_{opt} is the optimum microalgae growth temperature, and E_a is the activation energy

carboxylation Rubisco. Now the remaining problem is how to add the temperature function to the ordinary differential functions. The temperature function can be added to Bernard's model [20] by assuming the nitrogen uptake rate and the average growth rate to be related to the temperature factor. The equations of modified model of Bernard's are

$$\dot{s} = Ds_{in} - \overline{\rho}\frac{s}{s+K_s}\left(1-\frac{q}{Q_1}\right)f(T)x - Ds \quad (36)$$

$$\dot{q} = \overline{\rho}\frac{s}{s+K_s}\left(1-\frac{q}{Q_1}\right)f(T) - \overline{\mu}(I_0, I^*, x, q)(q-Q_0)f(T) \quad (37)$$

$$\dot{x} = \overline{\overline{\mu}}(I_0, I^*, x, q)\left(1-\frac{Q_0}{q}\right)f(T)x - Dx - Rf(T)x \quad (38)$$

When the environmental temperature T is equal to the optimum temperature T_{opt}, the temperature function $f(T)=1$, thus the model will degenerate to Bernard's model.

In Quinn et al.'s model [18], the temperature factor is taken into consideration. Substituting temperature function into Eqs. (20), (27) and (28), the below equations are derived

$$\rho(s,q) = \overline{\rho}\frac{s}{s+K_s}\left(1-\frac{q}{Q_1}\right)f(T) \quad (39)$$

$$p_m = p^C_{ref}\left(\frac{q-Q_0}{Q_1-Q_0}\right)f(T) \quad (40)$$

$$p_m = p^C_{ref}\left(1-\frac{Q_0}{q}\right)f(T) \quad (41)$$

Based on Bernard's model [20], a modified Quinn et al.'s model [18] is established whose growth part and temperature function are substituted by Eqs. (39)–(41) in Quinn et al.'s model. The model will be discussed in the next part.

Geider et al. [17] also took temperature effect into consideration in nitrogen uptake, as shown in Eq. (23). Packer et al. [19] didn't take the temperature factor into consideration in their model.

3. Results and discussion

Fig. 1 compares the simulations using this model and the experimental data about *Isochrysis galbana* performed by Flynn et al. [21]. The parameters used in the simulations with the model are presented in Table 1. It is assumed that no additional nutrition is added into the culture once the growth of microalgae began. As shown in Fig. 1, the model simulations have a good agreement with the experiment data [21], which shows the validation of the simulations. This figure indicated that the extracellular nitrogen was exhausted on the 12th day. At the same time, the synthesis of chlorophyll ceased. The growth process of biomass content with time could be divided into four phases [21]. The first five days were the lag phase, during which the cells increased at a slow rate. Following the lag phase was the exponential phase (from the 5th day to the 12th day), during which the growth rate of cells was 0.4 day^{-1}. The cells didn't stop growing until the 19th day, and these days (from the 12th day to the 19th day) were the post-exponential phase. After that, the culture entered the stationary phase, during which the content of biomass, chlorophyll and intracellular nitrogen were stable.

3.1. Light distribution modelling

In order to illuminate the influence of various light distribution relationships on the simulation results, simulations based on Bernard's model by using different expressions of the light attenuation coefficient ξ are performed and compared.

The simulations show that, for $L=0.05$ m, compared with light distribution sub-models proposed by Quinn et al.'s [18] and Packer et al.'s model [19], the chlorophyll values for sub-models from Bernard's model [20] and Geider et al.'s model [17] are a bit lower in algae biomass concentration while the inorganic nitrogen concentration, chlorophyll concentration and intracellular nitrogen concentration are almost the same. Things are different when the reactor becomes deeper. When $L=0.5$ m, the differences of the four curves corresponding to the four expressions of the light attenuation coefficient ξ become obvious though their variation

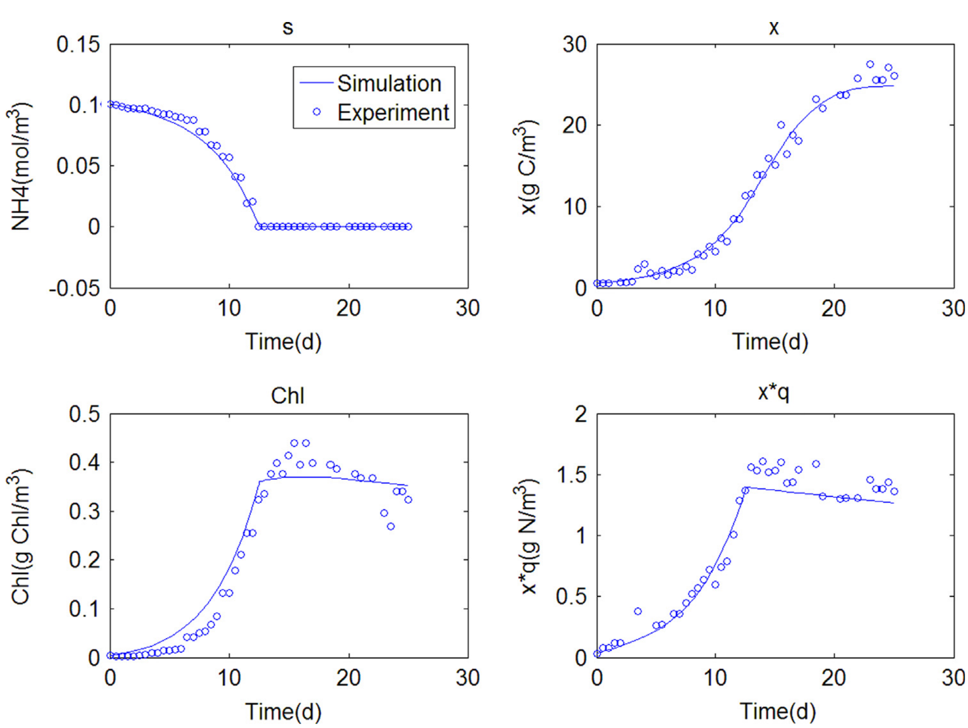


Fig. 1. Comparison of simulation and experimental data from [21].

trends with time are the same. Compared with light distribution sub-models proposed by Quinn et al.'s [18] and Packer et al.'s model [19], the growth rate and nitrogen uptake rate results for sub-models from Bernard's model [20] and Geider et al.'s model [17] are lower while the chlorophyll content is even larger.

3.2. Pigment dynamics modelling

Simulations based on Bernard's model [20] by using different expressions of the chlorophyll content are performed and compared. Fig. 2 shows that the variations of four main parameter values with time calculated based on Bernard's model by using three different expressions of the chlorophyll concentration *Chl* when $L=0.05$ m.

Table 1
Parameters values used in simulation.

Parameters	Values	Units
$\tilde{\mu}$	1.7	Day^{-1}
Q_0	0.05	g N (g C)^{-1}
Q_1	0.25	g N (g C)^{-1}
K_{sI}^*	1.4	$\text{mol m}^{-2}\,\text{s}^{-1}$
K_{iI}	295	$\text{mol m}^{-2}\,\text{s}^{-1}$
$\bar{\rho}$	0.073	$\text{g N (g C)}^{-1}\,\text{day}^{-1}$
K_s	0.0012	g N m^{-3}
R	0.0081	Day^{-1}
$\gamma_{\max}$	0.68	$\text{g } Chl\text{ (g N)}^{-1}$
k_{I^*}	63	$\text{mol m}^{-2}\,\text{s}^{-1}$
α^{Chl}	0.46	$\text{m}^2\text{ (g } Chl)^{-1}$
I_0	100	$\text{mol m}^{-2}\,\text{s}^{-1}$
ζ	2.0	g C (g N)^{-1}
$\theta^N_{\max}$	0.3	$\text{g } Chl\text{ (g N)}^{-1}$
p^C_{ref}	3.0	Day^{-1}
C_0	0.61	g C (g dw)^{-1}
A	4.82	$\text{m}^2\,\text{g}^{-1}\,Chl$
Φ	9.84×10^{-2}	$\text{g C (mol photons)}^{-1}$
E_a	63	kJ mol^{-1}
R_0	8.3145	$\text{J K}^{-1}\,\text{mol}^{-1}$
T_{opt}	18	°C

As shown in Fig. 2, the dissolved nitrogen concentration, and the carbon and nitrogen contents for different pigment sub-models are almost the same expect chlorophyll content. Fig. 3 shows the four main parameter values when L changes to 0.5 m. The differences in inorganic nitrogen concentration, intracellular carbon concentration and intracellular nitrogen concentration results of different pigment sub-models appear and the differences between the chlorophyll content are still evident.

3.3. Nitrogen uptake modelling

Fig. 4 shows that the variations of four main parameter values which is same as Fig. 2 with time calculated based on Bernard's model by using three different expressions of the nitrogen uptake when $L=0.05$ m. The chlorophyll content, intracellular carbon concentration and intracellular nitrogen concentration result for nitrogen uptake sub-models from Geider et al.'s model [17] is smaller than the sub-models from Bernard's model [20] and Quinn et al.'s model [18] while the inorganic nitrogen concentration is almost the same.

3.4. Growth rate modelling

Fig. 5 shows that the variations of four main parameter values which is same as Fig. 2 with time calculated based on Bernard's model by using four different expressions of the growth rate when $L=0.05$ m. Note that parameter p^C_{ref} is selected as 35 day^{-1} in Geider et al.'s model and 30 day^{-1} in Quinn et al.'s model.

As seen from Fig. 5, it is concluded that the four curves have the same trend. The growth rate for growth sub-models from Geider et al.'s model [17] and Quinn et al.'s model [18] are drastically larger than the sub-models from Bernard's model [20] and Packer et al.'s model [19] after the fourth day. But the inorganic nitrogen concentration, chlorophyll content and intracellular nitrogen concentration result for growth sub-models from four references approximate to each other.

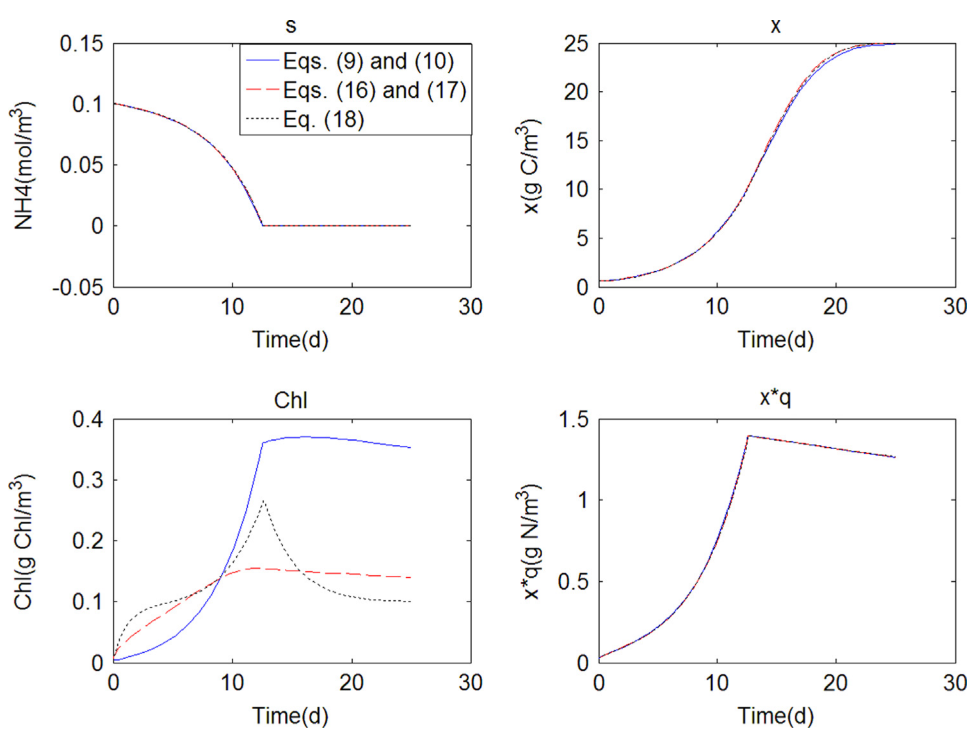


Fig. 2. Three different expressions to calculate the chlorophyll content when $L=0.05$ m.

3.5. Respiration rate modelling

Fig. 6 shows that the variations of four main parameter values calculated based on Bernard's model [20] by using five different expressions of the respiration rate when $L=0.05$ m. Based on Bernard's model, the respiration parts in every equations are added in Eqs. (2) and (3). The five cases are analyzed as follows: (1) adding $-Rx$ into Eq. (3), where $R=0.0081$ day^{-1}; (2) assuming $R=0$; (3) adding $-R_C x$ into Eq. (3), where $R_C=4.32\times10^{-4}$ day^{-1}; (4) adding $-Rx$ in Eqs. (2) and (3), where $R=0.0081$ day^{-1}; and (5) calculating the factor R with Eq. (33).

As shown in Fig. 6, the growth rate for respiration sub-model proposed by Mairet et al. [22] is a bit smaller than the sub-models from the other four. In general, the respiration factor is not an important aspect in the whole model, but an accuracy method is necessary if we want to get a better result.

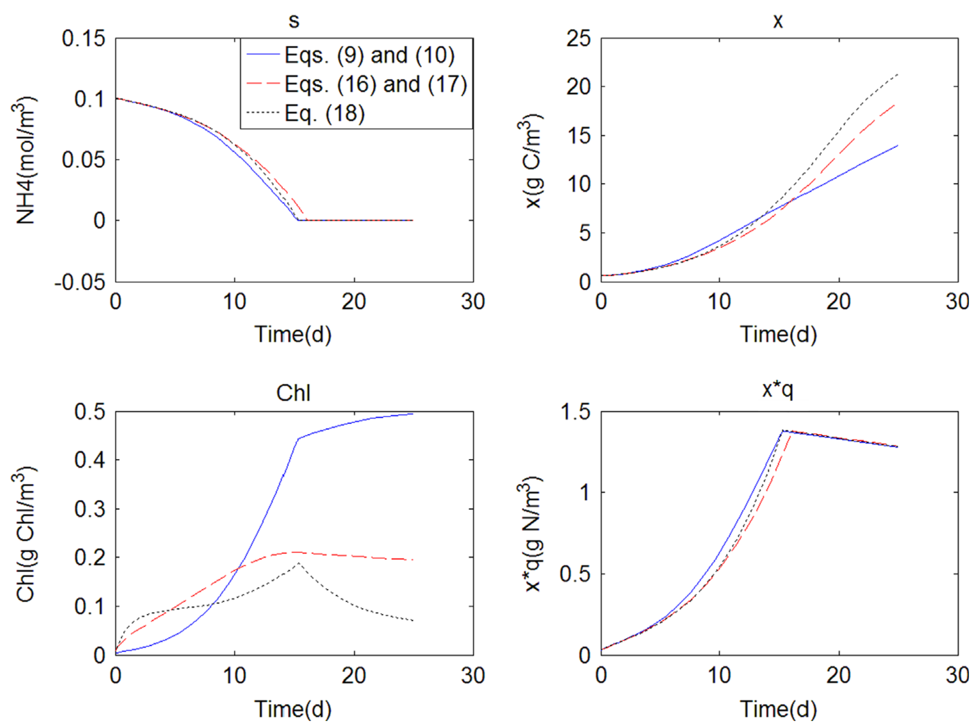


Fig. 3. Three different expressions to calculate the chlorophyll content when $L=0.5$ m.

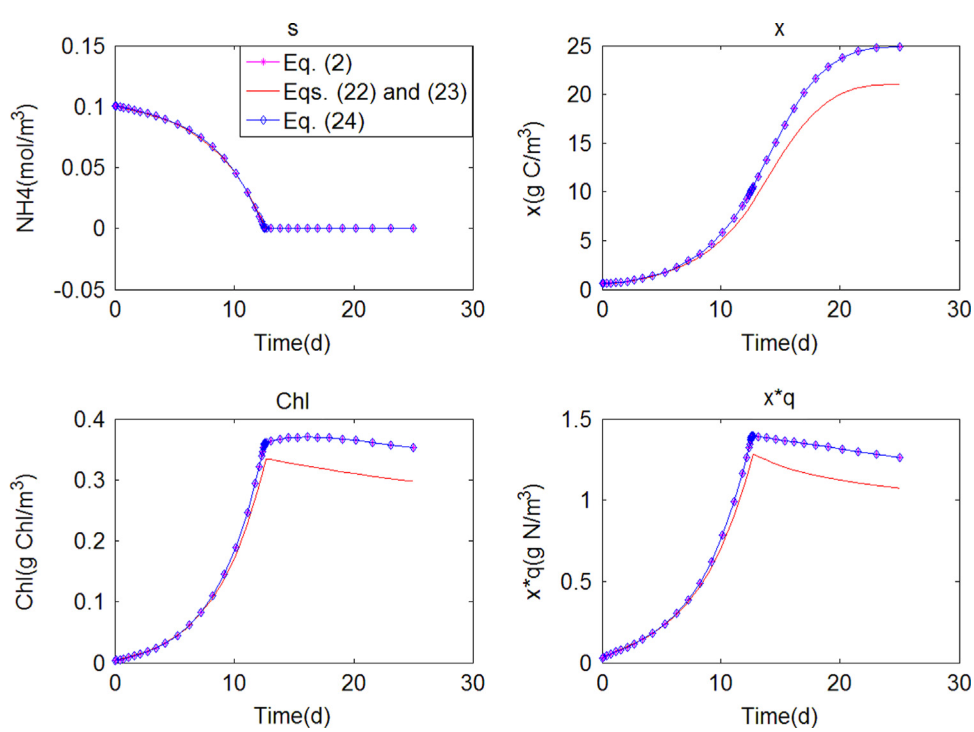


Fig. 4. Four main parameter values calculated based on Bernard's model by using three expressions of nitrogen uptake when $L=0.05$ m.

3.6. Depth dependence modelling

In this paper, the depths of bioreactor, L, are 0.05 m and 0.5 m, which represent the shallow bioreactors and the deep bioreactors, respectively. The variations of the four parametric values with different depths are discussed and compared in Fig. 7. As shown in Fig. 7, the results of four main parametric values vary a little with the depth when the depth L varies from 0.03 m to 0.15 m. This shows that it is reasonable to take L=0.05 m as a reference example to represent the shallow depth in this paper. Fig. 8 shows four parametric values vary with time when the bioreactors become deeper. The results of four main values vary a lot with the depth when the depth L varies from 0.05 m to 1.00 m. When L=1.00 m, not only the biomass concentration become lower, but

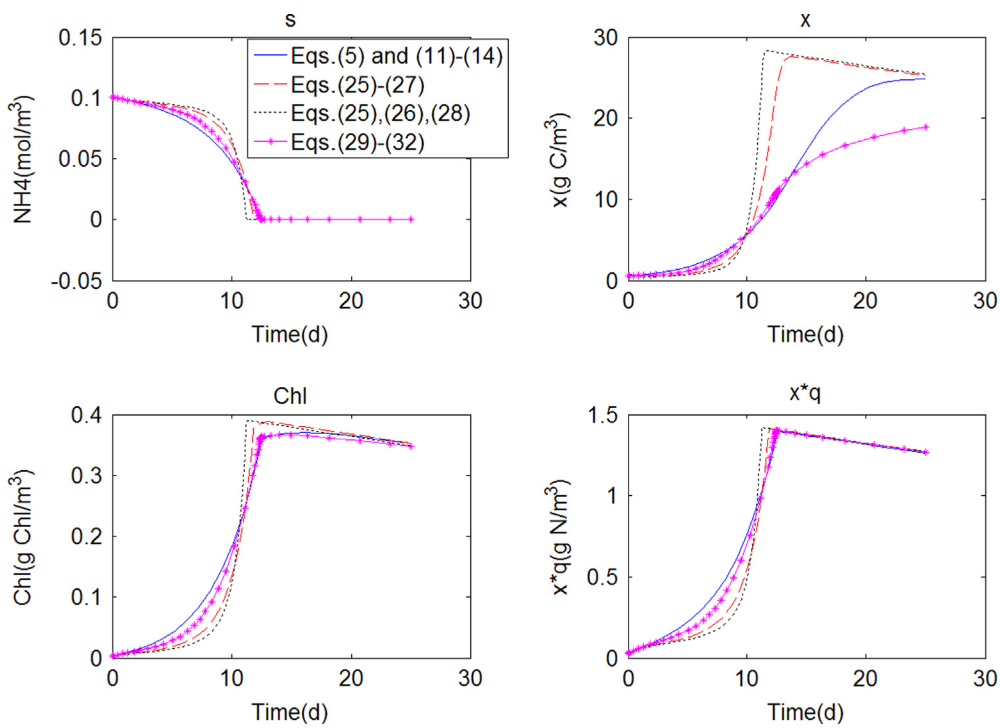


Fig. 5. Four main parameter values calculated based on Bernard's model by using four different expressions of growth rate when L=0.05 m.

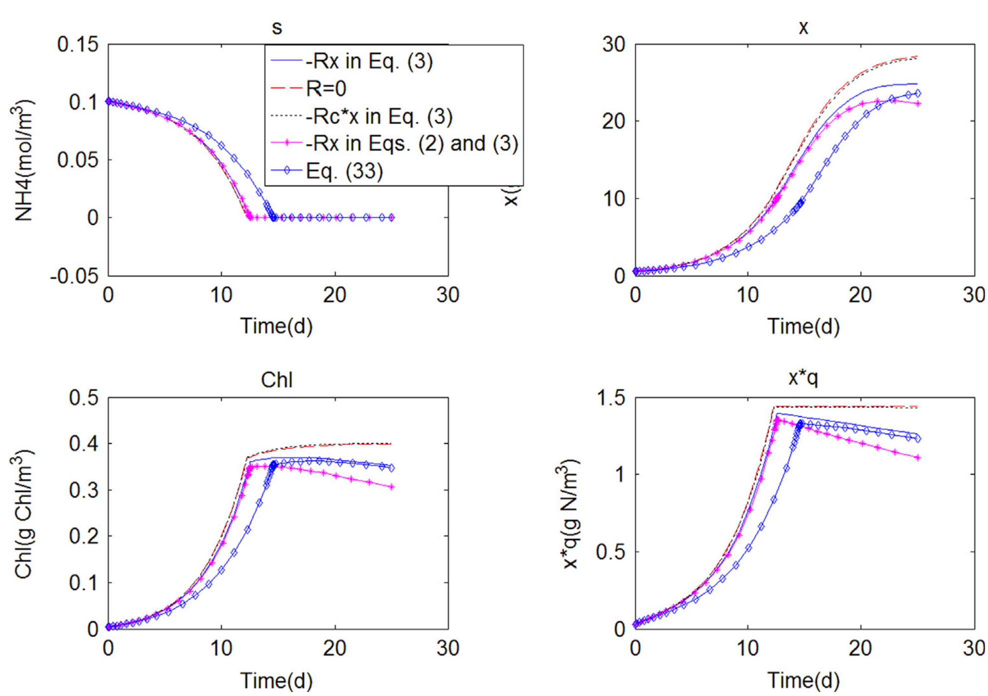


Fig. 6. Four main parameter values calculated based on Bernard's model by using five different expressions of the respiration rate when L=0.05 m. The five expressions are: (1): adding $-Rx$ into Eq. (3), where R=0.0081 day^{-1}; (2): assuming R=0; (3): adding $-R_C x$ into Eq. (3), where R_C=4.32×10^{-4} day^{-1}; (4): adding $-Rx$ in Eqs. (2) and (3), where R=0.0081 day^{-1}; (5): calculating the factor R with Eq. (33).

also more materials such as nitrate are demanded. Compared these two figures, it is found out that the biomass concentration will decrease a lot when the PBR depth is larger than 0.15 m.

3.7. Temperature dependence modelling

Fig. 9 shows that the variations of four main parametric values calculated based on the modified Bernard's model [20] by using five different temperature rates when $L=0.05$ m. As shown in Fig. 9, based on the assumption of the optimal temperature of 18 °C for *Isochrysis galbana,* the modified Bernard's model is degenerated to Bernard's model without considering the temperature factor. Although there are same trends for all the five curves at various temperatures ($T=8$, 16, 18, 20, and 28 °C), microalgae grow slower when the environment temperature is deviated from the optical temperature of the algae.

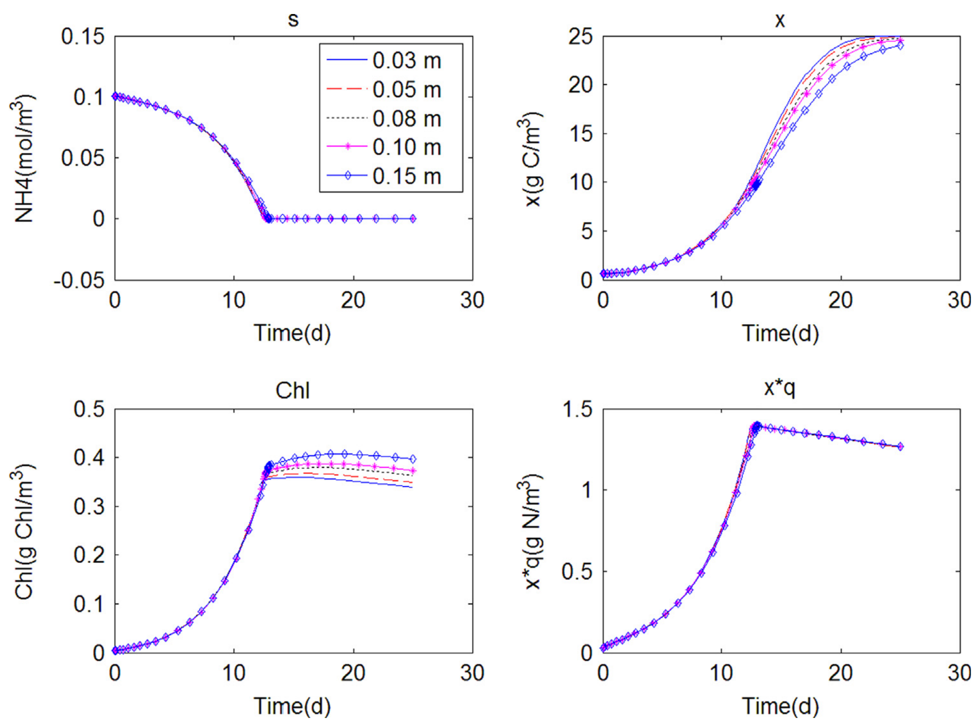


Fig. 7. Four main parameter values calculated based on Bernard's model by using four different expressions at five depths ($L=0.03$ m, 0.05 m, 0.08 m, 0.10 m, 0.15 m).

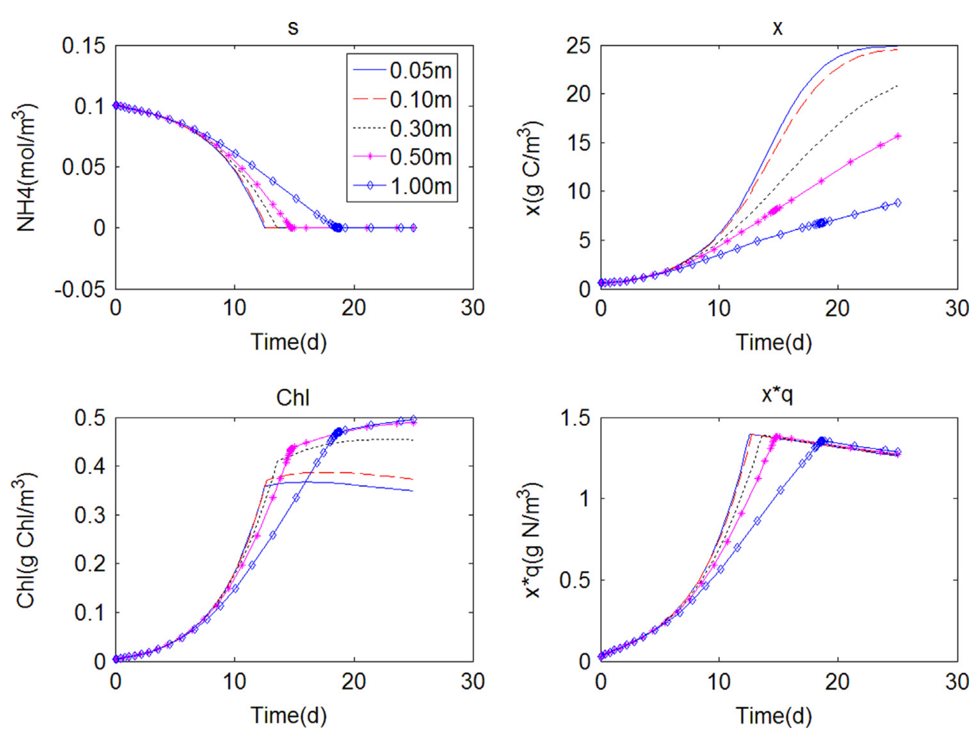


Fig. 8. Four main parameter values calculated based on Bernard's model by using four different expressions at five depths ($L=0.05$ m, 0.10 m, 0.30 m, 0.50 m, and 1.00 m).

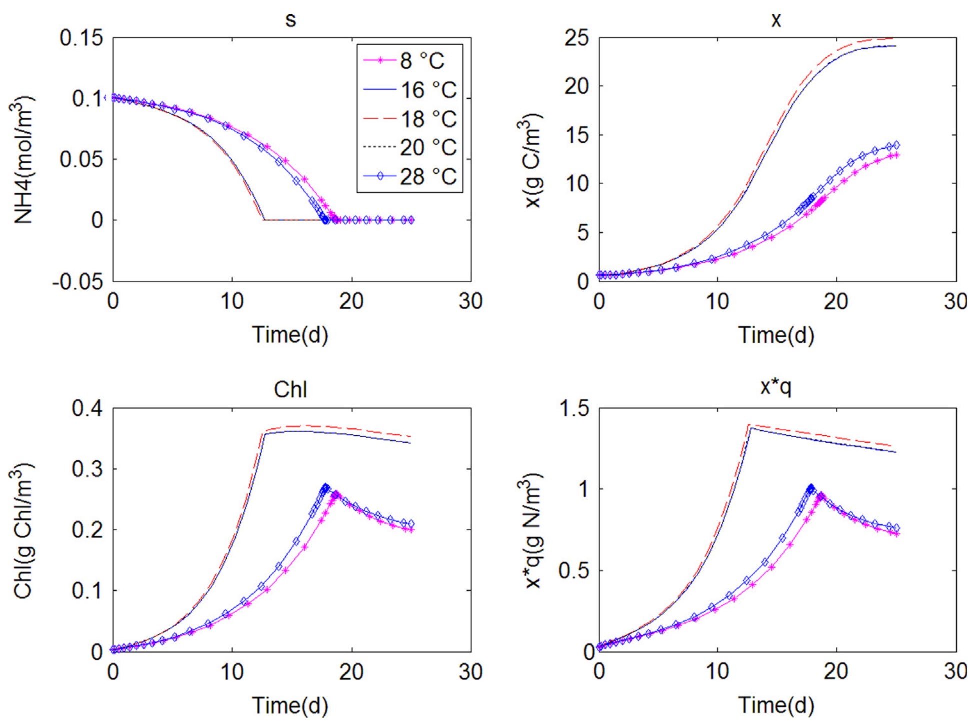


Fig. 9. Four main parameteric values calculated based on modified Bernard's model at five different temperatures.

4. Conclusions

Microalgae acted as the second generation biofuels could be produced in quantity with culture technologies in artificial bioreactors. Modelling microalgae growth is an effective method to predict the growth process, and then estimate the production and help to improve the productivity of microalgae under a given culturing condition at a given site. Recently, some models have been proposed with various expressions and coefficients of parameters. In this paper, the differences due to use of the various expressions and coefficients of parameters in the models have been compared. The conclusions are drawn (based on the case L=0.05 m) as follows:

(1) Compared with light distribution sub-models proposed by Quinn et al.'s [18] and Packer et al.'s model [19], the chlorophyll values for sub-models from Bernard's model [20] and Geider et al.'s model [17] are a bit lower in algae biomass concentration. The inorganic nitrogen concentration, intracellular carbon concentration and intracellular nitrogen concentration results of different pigment sub-models are almost the same expect chlorophyll content.
(2) The chlorophyll concentration, intracellular carbon concentration and intracellular nitrogen concentration result for nitrogen uptake sub-models from Geider et al.'s model [17] is smaller than the sub-models from Bernard's model [20] and Quinn et al.'s model [18] while the inorganic nitrogen concentration is almost the same.
(3) The growth rate for growth sub-models from Geider et al.'s model [17] and Quinn et al.'s model [18] are drastically larger than the sub-models from Bernard's model [20] and Packer et al.'s model [19] after the fourth day. The growth rate for respiration sub-model proposed by Mairet et al. [22] is a bit smaller than the sub-models from the other four.
(4) It is concluded that the biomass concentration will decrease a lot when the PBR depth is larger than 0.15 m. Microalgae grow slower when the environment temperature is deviated from the optimum temperature of the algae.

This paper will guide the researchers to select the most appropriate models or sub-models or build new models in order to model the microalgae growth process.

Nomenclature

A	optical cross section of chlorophyll a ($m^2\ g^{-1}\ Chl$)
C_0	carbon subsistence quota ($g\ C\ (g\ dw)^{-1}$)
Chl	chlorophyll concentration ($g\ Chl\ (g\ dw)^{-1}$)
D	dilution rate (day^{-1})
E_a	activation energy carboxylation Rubisco ($J\ mol^{-1}$)
$f(T)$	temperature function (Dimensionless)
F	nitrogen restriction factor (Dimensionless)
h_{Chl}	chlorophyll a synthesis regulation term (Dimensionless)
I_0	light intensity at reactor surface ($mol\ m^{-2}\ s^{-1}$)
I_{opt}	radiation providing maximal rate of photosynthesis ($mol\ m^{-2}\ s^{-1}$)
$I^*(t)$	conceptual radiation ($mol\ m^{-2}\ s^{-1}$)
$\bar{I}$	average radiation along culture volume ($mol\ m^{-2}\ s^{-1}$)
L	depth of culture (m)
p	photosynthesis rate (day^{-1})
p_m	maximum value of p at temperature T (day^{-1})
p^C_{ref}	maximum photosynthesis rate (day^{-1})
$q(t)$	internal nitrogen cell quota ($g\ N\ (g\ C)^{-1}$)
Q_0	minimum nitrogen quota ($g\ N\ (g\ C)^{-1}$)
Q_1	maximum nitrogen quota ($g\ N\ (g\ C)^{-1}$)
R	respiration rate (day^{-1})
R_0	universal gas constant ($J\ K^{-1}\ mol^{-1}$)
R_C	maintenance respiration rate (day^{-1})
r_{Chl}	chlorophyll a degradation rate constant (day^{-1})
r_N	nitrogen remineralization rate constant (day^{-1})
R_N	respiration constant for nitrogen (day^{-1})
$s(t)$	concentration of dissolved inorganic nitrogen, (nitrate or ammonium) ($g\ N\ m^{-3}$)
S_{in}	influent inorganic nitrogen concentration ($g\ N\ m^{-3}$)
T_{opt}	optimum growth temperature (°C)
$x(t)$	biomass concentration ($g\ C\ m^{-3}$)

α^{Chl} chlorophyll a-specific initial slope of photosynthesis-light curve ($m^2\,(g\,Chl)^{-1}$)
$\gamma(I^*)$ proportional coefficient of Chlorophyll concentration: nitrogen concentration ($g\,Chl(g\,N)^{-1}$)
γ_{max} maximum value of $\gamma(I^*)$ ($g\,Chl\,(g\,N)^{-1}$)
ζ cost of biosynthesis ($g\,C\,(g\,N)^{-1}$)
θ_0^C initial value of θ^C ($g\,Chl\,(g\,C)^{-1}$)
θ^C chlorophyll a: phytoplankton carbon ratio ($g\,Chl\,(g\,C)^{-1}$)
θ^N maximum chlorophyll a: N ($g\,Chl\,(g\,N)^{-1}$)
θ^N_{max} maximum value of θ^N ($g\,Chl\,(g\,N)^{-1}$)
λ optical depth (Dimensionless)
μ growth rate (day^{-1})
$\overline{\overline{\mu}}$ average growth rate (day^{-1})
$\tilde{\mu}$ maximal growth rate (day^{-1})
ξ light attenuation rate (m^{-1})
ρ uptake rate of nitrogen ($g\,N\,(g\,C)^{-1}\,day^{-1}$)
$\overline{\rho}$ maximum nitrogen absorption rate ($g\,N\,(g\,C)^{-1}\,day^{-1}$)
Φ Quantum efficiency ($g\,C\,(mol\,photons)^{-1}$))

Acknowledgement

This research has been partially supported by the National Natural Science Foundation of China (No. 50908094), the Ph.D. Programs Foundation of Ministry of Education of China (No. 20100142120071), the Fundamental Research Funds for the Central Universities, HUST (No. 2013NY015), and the Guangdong Province Enterprises Universities Researches Cooperation Major Project (No. 2012A090300012).

References

[1] Zhou XP, Wang F, Hu HW, Yang L, Guo PH, Xiao B. Assessment of sustainable biomass resource for energy use in China. Biomass Bioenergy 2011;35:1–11.
[2] Chisti Y. Biodiesel from microalgae beats bioethanol. Trends Biotechnol 2008;26:126–31.
[3] Zhou XP, Yuan S, Wu C, Song B, Peng SL. Potential production and distribution of microalgae in China. J Renew Sust Energ Rev 2013;5:053101.
[4] Oswald WJ, Golueke CG. Biological transformation of solar energy. Adv Appl Microbiol 1960;2:223–62.
[5] Burris JE. Photosynthesis, photorespiration, and dark respiration in eight species of algae. Mar Biol 1977;39:371–9.
[6] Laws E, Bannister T. Nutrient and light limited growth of *Thalassiosira fluviatilis* in continuous culture with implications for phytoplankton growth in the ocean. Limnol Oceanogr 1980;25:457–73.
[7] Hu Q, Richmond A. Productivity and photosynthetic efficiency of Spirulina platensis as affected by light intensity, algal density and rate of mixing in a flat plate Photobioreactor. J Appl Phycol 1996;8:139–45.
[8] Stephenson AL, Kazamia E, Dennis JS, Howe CJ, Scott SA, Smith AG. Life-cycle assessment of potential algal biodiesel production in the United Kingdom: a comparison of raceways and air-lift tubular bioreactors. Energy Fuels 2010;24:4062–77.
[9] Demirbas A, Demirbas MF. Importance of algae oil as a source of biodiesel. Energy Convers Manage 2011;52:163–70.
[10] Huisman J, Weissing FJ. Light limited growth and competition for light in well mixed aquatic environments: an elementary model. Ecology 1994;75:507–20.
[11] Huisman J. Population dynamics of light-limited phytoplankton: microcosm experiments. Ecology 1999;80:202–10.
[12] Bernard O, Masci P, Sciandra A. A photobioreactor model in nitrogen limited conditions. In: Proceedings of the sixth conference on mathematical modelling, Vienna, 2009.
[13] Cherif M, Loreau M. Towards a more biologically realistic use of Droop's equations to model growth under multiple nutrient limitation. Synth Ecol 2010;119:897–907.
[14] Malthus TR. Essai sur le principe de population. Éditions Gonthier, Paris, 1798.
[15] Droop M. Vitamin B12 and marine ecology. IV. The kinetics of uptake, growth and inhibition in Monochrysis Lutheri. J Mar Biol 1968;48:689–733.
[16] Droop M. 25 Years of algal growth kinetics, a personal view. Botanica 1983;16:99–112 (Mar).
[17] Geider RJ, MacIntyre HL, Kana TM. A dynamic regulatory model of phytoplanktonic acclimation to light, nutrients, and temperature. Limnol Oceanogr 1998;43:679–94.
[18] Quinn J, de Winter L, Bradley T. Microalgae bulk growth model with application to industrial scale systems. Bioresour Technol 2011;102:5083–92.
[19] Packer A, Li Y, Andersen T, Hu Q, Kuang Y, Sommerfeld M. Growth and neutral lipid synthesis in green microalgae: a mathematical model. Bioresour Technol 2011;102:111–7.
[20] Bernard O. Hurdles and challenges for modeling and control of microalgae for CO_2 mitigation and biofuel production. J Process Control 2011;21:1378–89.
[21] Flynn KJ, Davidson K, Leftley JW. Carbon–nitrogen relations at whole-cell and free-amino-acid levels during batch growth of *Isochrysis galbana* (Prymnesiophyceae) under conditions of alternating light and dark. Mar Biol 1994;118:229–37.
[22] Mairet F, Bernard O, Lacour T, Sciandra A. Modeling microalgae growth in nitrogen limited photobiorector for estimating biomass, carbohydrate and neutral lipid productivities. In: The 18th IFAC world congress Milano, Italy; 2011.
[23] Hu Q, Sommerfeld M, Jarvis E, Ghirardi M, Posewitz M, Seibert M, et al. Microalgal triacylglycerols as feedstocks for biofuel production: perspectives and advances. Plant J 2008;54:621–63.
[24] Qiang H, Richmond A. Productivity and photosynthetic efficiency of *Spirulina platensis* as affected by light intensity, algal density and rate of mixing in a flat plate photobioreactor. J Appl Phycol 1996;8:139–45.
[25] Quinn JC, Catton K, Wagner N, Bradley TH. Current large-scale US biofuel potential from microalgae cultivated in photobioreactors. Bioenergy Res 2012;5:49–60.